Available online at www.sciencedirect.com
SCIENCE DIRECT
Journal of Power Sources 156 (2006) 472–479
JOURNAL OF POWER SOURCES
www.elsevier.com/locate/jpowsour

Analysis of stationary fuel cell dynamic ramping capabilities and ultra capacitor energy storage using high resolution demand data

James R. Meacham, Faryar Jabbari, Jacob Brouwer, Josh L. Mauzey, G. Scott Samuelsen *

National Fuel Cell Research Center (NFCRC), Advanced Power and Energy Program, University of California, Irvine, CA 92697-3550, USA

Received 1 May 2005; accepted 31 May 2005
Available online 8 September 2005

Abstract

Current high temperature fuel cell (HTFC) systems used for stationary power applications (in the 200–300 kW size range) have very limited dynamic load following capability or are simply base load devices. Considering the economics of existing electric utility rate structures, there is little incentive to increase HTFC ramping capability beyond 1 kWs^{-1} (0.4% s^{-1}). However, in order to ease concerns about grid instabilities from utility companies and increase market adoption, HTFC systems will have to increase their ramping abilities, and will likely have to incorporate electrical energy storage (EES). Because batteries have low power densities and limited lifetimes in highly cyclic applications, ultra capacitors may be the EES medium of choice. The current analyses show that, because ultra capacitors have a very low energy storage density, their integration with HTFC systems may not be feasible unless the fuel cell has a ramp rate approaching 10 kWs^{-1} (4% s^{-1}) when using a worst-case design analysis. This requirement for fast dynamic load response characteristics can be reduced to 1 kWs^{-1} by utilizing high resolution demand data to properly size ultra capacitor systems and through demand management techniques that reduce load volatility.

Keywords: Dynamic; Fuel cell; Ramping; Ultra capacitor; Load following

1. Introduction

Fuel cells exhibit efficiency and emissions characteristics that are enabling their penetration into the distributed power generation market and positioning them to be the preferred generation sources of the future. However, due to the high capital cost of fuel cell systems, adoption has not been widespread, with most installations occurring in niche applications with heavy subsidy [1]. The fuel cell systems deployed to-date are typically base load devices that do not allow dynamic load following, which can have drawbacks for both the end-user and utility grid. Recent demonstrations have shown the ramping capabilities of fuel cell systems to be less that 0.1% s^{-1} [2]. Because end-use loads are typically highly time-variant, fuel cells that do not have dynamic load following capability will not be used effectively in off-grid and grid outage situations, limiting their market appeal. In addition, base loaded fuel cells or fuel cells with limited ramping capabilities can impart large, intermittent spikes onto the utility grid (while reducing sustained power demand from the energy provider), a situation which will work to increase the resistance to fuel cell adoption by utility companies.

Fuel cells can be paired with electrical energy storage (EES) systems to increase their ability to meet dynamic loads, which will in turn help ease utility constraints and make fuel cells more marketable. However, the incorporation of EES into fuel cell systems will introduce increased system cost, complexity, and size, with the amount of EES needed varying greatly with the ramping rate of the fuel cell. There are two main types of EES available in the market today: batteries and ultra capacitors. Batteries have been used for decades in distributed (mostly renewable) power systems, and have high energy storage density and low power density relative to ultra capacitors. Batteries often require significant maintenance and have short lifetimes under highly cyclic applications. Ultra capacitors, on the other hand, have very long cycle lifetimes (over 100,000 cycles with minimal degradation), high

* Corresponding author. Tel.: +1 949 824 1999x120; fax: +1 949 824 7423.
E-mail address: gss@nfcrc.uci.edu (G.S. Samuelsen).

0378-7753/$ – see front matter © 2005 Elsevier B.V. All rights reserved.
doi:10.1016/j.jpowsour.2005.05.094

power densities, and high discharge and charge efficiencies which may be advantageous when combined with fuel cell systems [3,4].

Numerous studies have been carried out examining the dynamics of fuel cells paired with ultra capacitors for automotive applications; however, both fuel cell and end-use load dynamics are quite different in the context of stationary power applications [5,6]. Other studies have focused on the integration of fuel cells into residences for the design of ancillary devices such as inverters and converters, but do not use truly dynamic load data for performance or economic analyses [7,8].

Understanding the nature of end-use demand is critical to the design of fuel cell and EES systems. In most commercial environments, building electrical load data are collected in intervals of five minutes or longer (if at all). This averaging, however, does not capture the fast dynamics that fuel cell systems will be forced to address.

Additionally, typical economic analyses of fuel cell systems (such as the study by Archer et al. [9]) rely on daily averaged energy demands, resulting in an even greater loss of resolution and load dynamics, which have a profound impact on operations and utility pricing. As a result, high resolution building demand data are needed to adequately analyze the integration of fuel cell and ultra capacitor systems.

2. Analysis and model description

Dynamic models of distributed energy resource (DER) components are needed to simulate the fuel cell and ultra capacitor systems. Using Matlab® Simulink®, models of high temperature fuel cells, absorption chillers, electric chillers, ultra capacitors, and thermal energy storage have been developed for a wide array of analyses. Empirical models were constructed as individual modules for each of the major devices. Empirical models were used in order to reduce simulation time and ensure that the performance of each component would represent products in the marketplace. The component models were then integrated to simulate various system configurations, and applied to analyze the dynamic ramping capability of fuel cells and fuel cell ultra capacitor systems to meet the commercial office building load described in Section 2.3. The analysis is focused on understanding the amount of electrical energy storage required to meet the building demand for various fuel cell system ramp rates. Additionally, the economic and grid impacts of fuel cell systems with and without EES are analyzed for various fuel cell ramp rates.

2.1. Fuel cell model

Because high temperature fuel cells (HTFC) (such as molten carbonate fuel cells (MCFC) and solid oxide fuel cells (SOFC)) can operate directly on natural gas and have high fuel-to-electricity conversion efficiencies, they are positioned to gain the largest portion of the stationary fuel cell market. For that reason, the fuel cell used for this study is a generic high temperature fuel cell, with exhaust, efficiency, and performance characteristics of a system operating nominally at 650 °C. The model is driven by an efficiency curve derived from the only commercial HTFC product on the market today: FuelCell Energy's DFC300™, a 250 kW MCFC [10]. From this curve, thermodynamic analyses are used to determine the system operating conditions, and a linear power ramping rate equation is applied to govern the electrical dynamics. Because high temperature fuel cell systems will not be able to operate at very low partial loads, the fuel cell model is restricted to a minimum output of 100 kW (40% of rated output). The heat balance equation used to govern the fuel cell operating characteristics is shown below in Eq. (1).

$$\dot{Q}_{\text{fuel}} - \dot{Q}_{\text{electricity}} - \dot{Q}_{\text{reformation}} - \dot{Q}_{\text{losses}} - \dot{Q}_{\text{exhaust}} = 0 \tag{1}$$

where

$$\dot{Q}_{\text{fuel}} = \frac{P_{\text{HTFC}}}{\eta(P_{\text{HTFC}})}$$

$$\dot{Q}_{\text{electricity}} = P_{\text{HTFC}}$$

$$\dot{Q}_{\text{reformation}} = \frac{\dot{Q}_{\text{fuel}}\, h_{\text{reformation}}}{\text{LHV}_{\text{fuel}}}$$

$$\dot{Q}_{\text{losses}} = h_{SS}\, A_{\text{HTFC}}\, (T_{\text{HTFC}} - T_{\text{ambient}})$$

and P_{HTFC} is the power output of the fuel cell, $\eta(P_{\text{HTFC}})$ is the efficiency as a function of the fuel cell output power (as determined from the lookup table in reference [10]), $h_{\text{reformation}}$ is the heat needed for complete reformation of the fuel, LHV_{fuel} is the lower heating value of the fuel, h_{SS} is the convection coefficient of stainless steel, A_{HTFC} is the area of the fuel cell, T_{HTFC} is the operating temperature of the fuel cell as function of convective heat loss, power output, and heat loss due to reformation, and T_{ambient} is the ambient air temperature surrounding the fuel cell.

2.2. Ultra capacitor model

The ultra capacitor model used for this study is based on the previous work of New et al. [11]. The ultra capacitor is represented by a simple R-C circuit with three time constant components and a leakage resistance (Fig. 1). Additionally, a voltage regulator is used to maintain appropriate cell voltages as discussed below. Miller et al. [12] go on to extrapolate the single cell model to incorporate any number of cells in series, so that banks of ultra capacitors can be simulated. The resulting expressions governing the resistance and capacitance values for the three time constant components and leakage resistance in Fig. 1 are shown in Table 1. The Matlab Simulink™ ultra capacitor model utilized in this work was developed using this approach, and employs component characteristics for a commercial ultra capacitor available from

Table 1
Equations for three time components of ultra capacitor model

Fast		Medium		Slow		Leakage	
R_{fast}	$\frac{2N}{3}$ESR	R_{medium}	$\frac{2N}{3}\Phi^{-(2k-1)}$ESR	R_{slow}	$\frac{2N}{3}\Phi^{-(2k+1)}$ESR	R_{leak}	$950N$
C_{fast}	$\frac{1.05}{N}C_0$	C_{medium}	$\frac{1.05}{N}\Phi^{(2j+1)}C_0$	C_{slow}	$\frac{1.05}{N}\Phi^{(2j-1)}C_0$		

Note: N is the number of cells in series, ESR (equivalent series resistance) = 0.7mO, $F = 0.618$, $C_0 = 2600$F, $j = 2$ and $k = 8$.

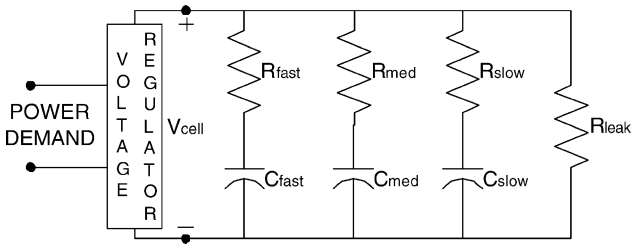

Fig. 1. R-C model of an ultra capacitor system.

Maxwell Technologies (BCAP0100® 2600 Farad, 2.5 V, currently costing about US$ 180 per cell).

The ultra capacitor system must be regulated, however, as the system voltage is highly variable, dependent on state of charge (SOC) and instantaneous power demand. Many wide-range DC–DC converters such as the design by Todorovic et al. [13] can readily handle a voltage variation of 2:1. As a result, the current ultra capacitor system model contains a voltage regulator that does not allow the individual cell voltages to drop below 1.25 V, or one half of the rated cell voltage. This restriction further limits the energy storage density of ultra capacitors, but is a realistic requirement for integrating ultra capacitors into building systems.

A representative charge/discharge cycle for a simulated ultra capacitor system containing 100 cells is shown in Fig. 2. Region I shows the charging region and the resulting drop in ultra capacitor charging power as the cell voltage approaches 2.5 V. This feature is necessary to protect the ultra capacitors from over charging, which quickly reduces cell lifetime. In Region II, the system is neither being charged nor discharged; the cell voltage drops during this time due to the leakage current (nominally 2.5 mA for this cell). In Region III of Fig. 2, the demand from the ultra capacitor system is increased to 10 kW; the system is able to meet this demand for approximately 50 s, until the cell voltage drops to the lower limit of 1.25 V.

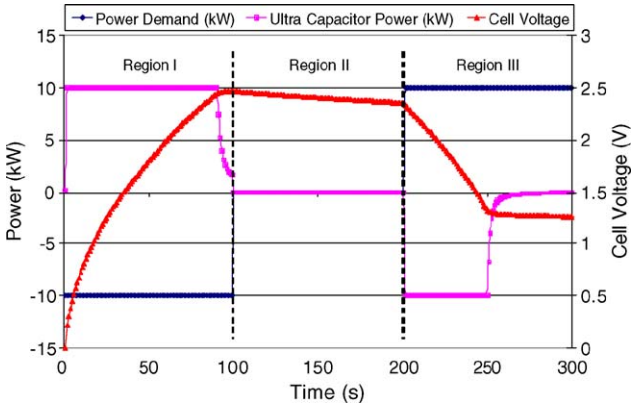

Fig. 2. Simulated charge/discharge cycle for a 100 ultra capacitor system.

This analysis shows that the usable energy storage of an individual ultra capacitor cells as currently simulated is approximately 1.8 Wh, which will be an important factor in determining the number of ultra capacitors needed as a function of fuel cell power ramp rate. Similar analyses show that each ultra capacitor cell modeled in this study has an instantaneous power density of approximately 1.4 kW (at a resting voltage of 2.35 V). Active charge control is used to maintain the ultra capacitor cell voltage between 2.3 and 2.4 V such that the EES will have the ability to both supply and accept power when needed.

2.3. Building electrical demand data

In order to examine the dynamics of fuel cell and ultra capacitor systems in the context of actual dynamic building demands, high resolution demand data have been gathered from a typical two story, 100,000 ft^2 commercial office building in Southern California. The high resolution data gathered for this study were collected in 3 s intervals, capturing fast transients otherwise lost by five minute averaged data. The dynamic load data were acquired using three high performance poly phase power meters (Dent Instruments ElitePro™ with extended memory). The current data were gathered using seven AC current transformers, with 3 Dent Instruments Flex3000L monitoring the 3-phase 480 V total building electricity demand and 4 Dent Instruments AC150a monitoring the building air conditioning circuits. Fig. 3 shows the differences between the 3 s and 5 min averaged data. When sampling at the typical 5-min interval, 20–40 kW step changes are replaced by smooth ramps, and some 40 kW spikes are missed altogether. These data emphasize the need for better time-resolved measurements for loads that are to be met by integrated fuel cells or other distributed generation systems. Because the utility rate schedules used for the majority of commercial buildings include a penalty for peak power demand, the use of averaged data could result in poor economic and performance analyses regarding integrated fuel cell systems.

Fig. 4 shows the 24 h load profile of the office building, which has a fairly typical diurnal cycle. The large step change seen at around 3 a.m. (~75 kW) results from the air

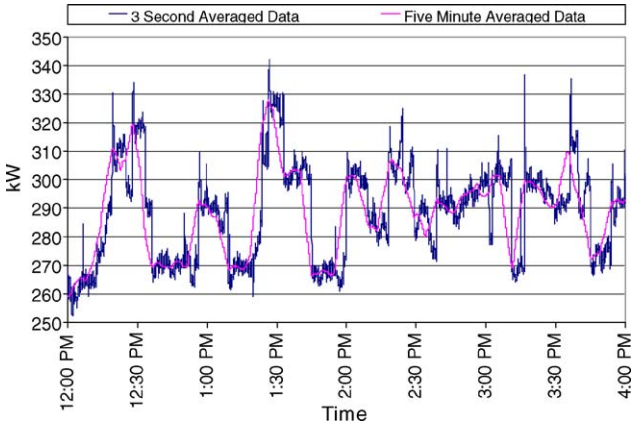

Fig. 3. Comparison of high-resolution and 5-min averaged data.

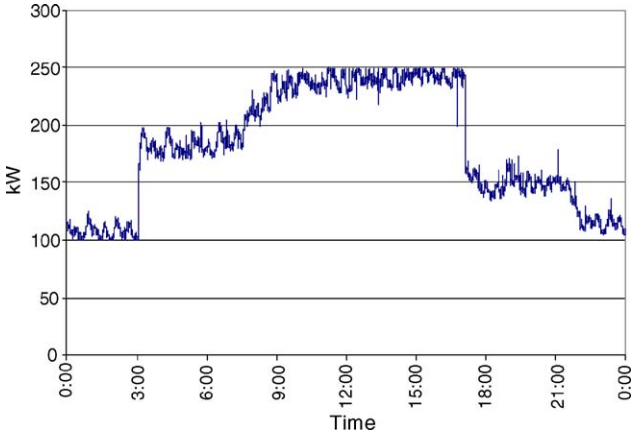

Fig. 4. High resolution building electrical demand used for analyses.

conditioning system coming on-line to begin cooling the building for the workday. The air conditioning system is turned off at 5 p.m. resulting in another large step change. The electrical demand remains fairly high in the evening and night as the company inhabiting the building has a large computational facility running 24 h a day. The building demand is limited to 250 kW (the capacity of the HTFC) in a manner that retains the dynamic performance requirements (i.e., inverting peak loads above 250 kW)to study EES as a function of fuel cell ramping rate without penalizing the HTFC for lack of overcapacity performance.

3. Simulation results

3.1. Fuel cell systems without ultra capacitors

The impact of varying ramp rates for fuel cell systems is first explored without integrating electrical energy storage. One day (24 h) of high resolution dynamic building load demand data (see Fig. 4) was used as the basis for all simulations conducted in this effort. Five different rising ramp rate capabilities were chosen for the fuel cell to investigate

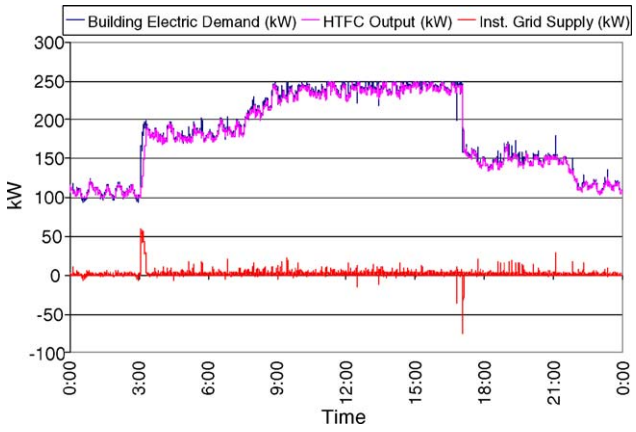

Fig. 5. Power data for 0.1 kWs^{-1} HTFC ramp rate.

the economic and grid impacts of fuel cell system integration into the commercial office building load described above. The fuel cell ramp rate capabilities simulated were 0.01, 0.1, 1.0, 10, and 100 kWs^{-1} (0.004, 0.04, 0.4, 4 and 40% s^{-1}). These rates encompass a wide range of ramping capability from virtually none to virtually instantaneous; for comparison, fuel cell ramp rates of 0.08% s^{-1} (equating to 0.2 kWs^{-1} for the system in this study) have been demonstrated in actual MCFC systems as described in the study by Leo et al. [2]. The falling ramp rate was chosen to be ten times faster than the rising ramp rate in all cases. This assumption is reasonable because load shedding in high temperature fuel cell systems is less difficult than ramping up power, although load shedding is not trivial and is highly dependent on system design. All results in this effort are presented in the context of grid-parallel operation. Any use of grid power is a direct result of the integrated fuel cell system inability to meet the dynamic load, and would thus be a shortfall in stand-alone operating mode.

Figs. 5 and 6 show the building electrical demand, HTFC output, and grid input for building-integrated fuel cell systems having ramp rates of 0.1 and 10 kWs^{-1}, respectively. A fuel cell ramp rate of 0.1 kWs^{-1} (0.04% s^{-1}) results in large

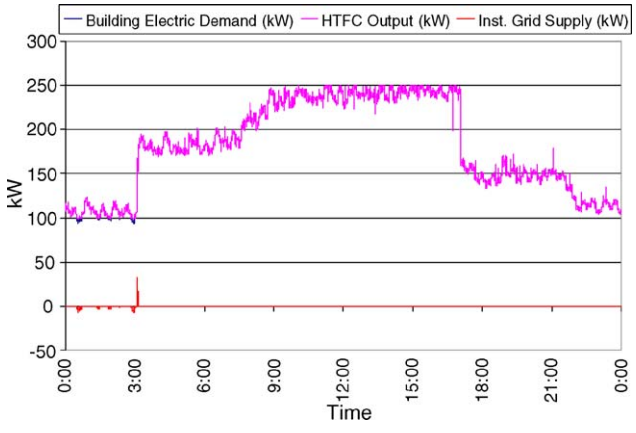

Fig. 6. Power data for 10 kWs^{-1} HTFC ramp rate.

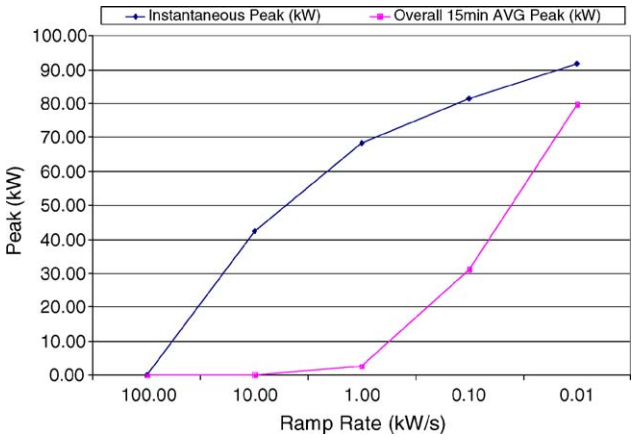

Fig. 7. Instantaneous and rolling average grid demand.

spikes to and from the grid and nearly continual perturbation, while a ramp rate of 10 kWs^{-1} (4% s^{-1}) significantly reduces the grid impact. Even with the very responsive ramp rate of 10 kWs^{-1}, however, a 42 kW instantaneous grid peak is generated. While this peak is quickly eliminated by the fuel cell system, it could still lead to local grid instabilities, especially if fuel cells become more pervasive in the marketplace.

Fig. 7 shows the instantaneous and rolling average grid demands as a function of HTFC ramp rate. The 15-min rolling average demand is interesting as this is typically the integration period used by utility companies when determining demand charges. Fig. 7 shows that the average demand (and utility charges for such) does not increase significantly until the ramp rate becomes slower than 1 kWs^{-1} (0.4%). Economically, this suggests that there is little incentive to increase the ramping rate beyond 1 kWs^{-1} for a grid-connected system, as illustrated in Fig. 8 (the 24-h operating costs in Fig. 8 are calculated using a natural gas cost of US$ 0.70 per therm and the SCE GS-2 electric utility rate schedule). Although the economics for this case do not suggest increasing the fuel cell ramp rate beyond 1 kWs^{-1}, the instantaneous grid supply peaks remain significant for any fuel cell ramping rate slower

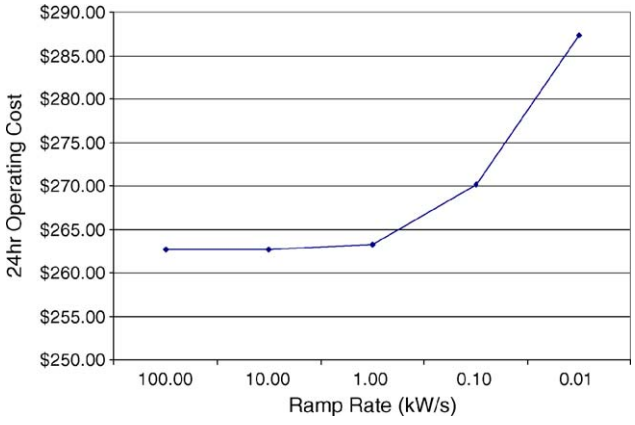

Fig. 8. 24 h operating cost as a function of HTFC ramping rate.

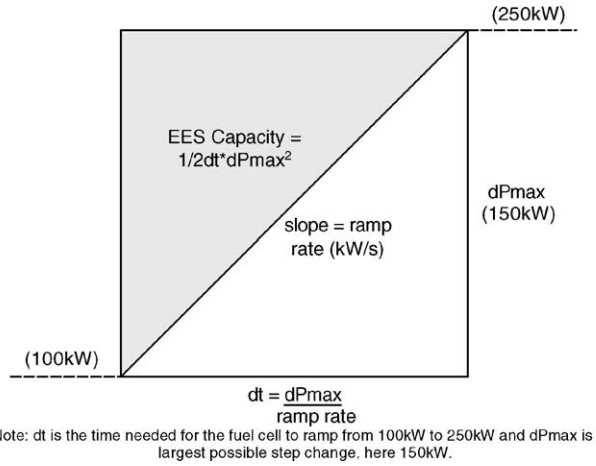

Note: dt is the time needed for the fuel cell to ramp from 100kW to 250kW and dPmax is the largest possible step change, here 150kW.

Fig. 9. Worst-case EES capacity calculation—linear integration.

than 100 kWs^{-1} (Fig. 7), creating grid instability issues for both utilities and end-users to consider.

3.2. Fuel cell systems with ultra capacitors

In order to investigate the dynamics of integrated fuel cell ultra capacitor systems, the size of the ultra capacitor bank must first be determined for each HTFC ramping rate. Design of the ultra capacitor EES is a complex process that is highly dependent on the variability of the end-use load. For this study, a worst case scenario analysis is used as a starting point. The maximum amount of EES is needed when the HTFC is stepped from its lowest power level (100 kW) to its maximum output (250 kW). Because the ramping rates of the HTFC are assumed linear, simple linear integration can be used to determine the amount of energy storage needed by calculating the area of the triangle defined by the ramp rate and maximum power change (see Fig. 9). The maximum EES capacities (in kWh and number of ultra capacitor cells) as a function of HTFC ramping rate are plotted in Fig. 10. The amount of EES is relatively small until the ramp rate decreases below 10 kWs^{-1} (4% s^{-1}). This is an important point when considering the use of ultra capacitors as the EES

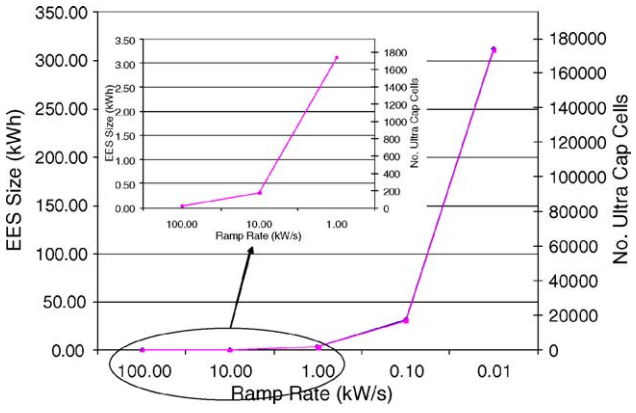

Fig. 10. Maximum EES capacity as a function of HTFC ramp rate.

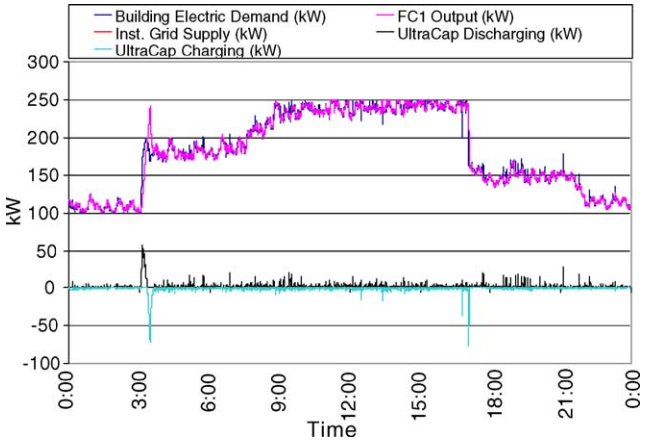

Fig. 11. Electrical outputs for 0.1 kWs^{-1} HTFC ramp rate with ultra capacitors.

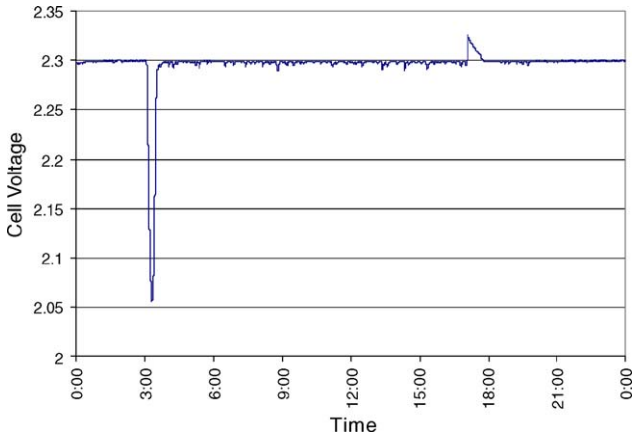

Fig. 12. Ultra capacitor cell voltage for 0.1 kWs^{-1}—worst-case sizing scenario.

medium, as their energy storage capacity is very small (here, 1.8 Wh $cell^{-1}$). At 1 kWs^{-1}, 1736 cells would be needed to fulfill the worst case scenario (150 kW step change), making ultra capacitors an impractical option for most applications. The exponential rise in the number of cells needed to compensate for the slow HTFC ramping rates suggests that ultra capacitors will not be a viable option if stationary fuel cells do not have at least a 10 kWs^{-1} (4% s^{-1}) slew rate (174 cells, based on worst case scenario analysis).

Not only must the ultra capacitor system be able to supply the necessary amount of energy to assist the fuel cell during the step change, the system must also be able to meet the instantaneous demand peak (here, 150 kW). Therefore, each ultra capacitor system must have a minimum of 108 cells; for the worst-case system sizing described above, this only affects the 100 kWs^{-1} system, which would otherwise have only included 18 cells.

The same five simulations presented above for the case without ultra capacitors (Section 3.1) were performed for each of the integrated fuel cell ultra capacitor systems to determine whether the grid peaks could be eliminated for a real, dynamic building load. In all cases, the EES system (sized using the worst-case scenario described above) allowed the system to operate with no grid perturbations, verifying that stand-alone operation could also be achieved. The results for the 0.1 kWs^{-1} case are shown in Fig. 11 as an example of the integrated fuel cell ultra capacitor system performance; note that there is no longer any power supplied to or from the grid. The ultra capacitor cell voltage, plotted in Fig. 12, dips only to about 2 V for this and all cases, suggesting that the EES system is over-sized for this particular load profile, because there is excess energy stored in the cells that is never used (the minimum cell operating voltage is 1.25 V).

4. Discussion

The analyses indicate that increasing fuel cell ramp rate is important for the reduction of grid impacts, which is accomplished primarily by reducing power spikes (both positive and negative) through faster dynamic responses to real load perturbations. In addition, the integrated use of fuel cells and banks of ultra capacitors was shown to eliminate grid perturbations and allow for stand alone operation of the fuel cell system to meet real dynamic load profiles. This capability, however, came at the significant cost of a very large bank of ultra-capacitors that may make these systems impractical.

Recognizing that the worst-case analysis used to design the ultra capacitor EES may not be necessary (or practical) for all fuel cell systems, five additional integrated systems were designed and simulated with smaller EES. In each case the ultra capacitor EES was sized to meet 120% of the difference between the demand (shown in Fig. 4) and the HTFC power capability for each ramp rate case. In all cases, this sizing scheme results in an EES designed to meet the dynamics of the ~3 a.m. air conditioning system start-up. The EES capacity (in kWh and number of cells) for the demand sizing method is presented in Fig. 13. It is important to note the significant reduction in EES size at 1 kWs^{-1} from the worst-case analysis, as the required number of cells is reduced from 1737 to 406. In all simulations, the integrated fuel cell systems with smaller EES are able to eliminate the utility grid

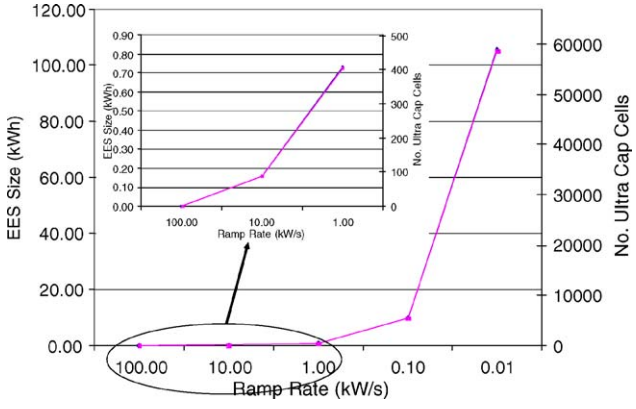

Fig. 13. Demand-estimated EES capacity as a function of HTFC ramp rate.

Table 2
Economic comparison HTFC—ultra capacitor ramp rates and system sizes

Ramp rate ($kW\,s^{-1}$)	Worst case design scenario		Building demand sized scenario	
	HTFC system cost with UltraCaps (US$\,kw^{-1})	Increase in system cost with UltraCaps (%)	HTFC system cost with UltraCaps (US$\,kw^{-1})	Increase in system cost with UltraCaps (%)
100.0	4007.20	0.2	4000	0.0
10.0	4069.60	1.7	4035.6	0.9
1.0	4694.80	17.4	4162.4	4.1
0.1	10944.80	173.6	6178	54.5
0.01	73444.80	1736.1	27444.8	586.1

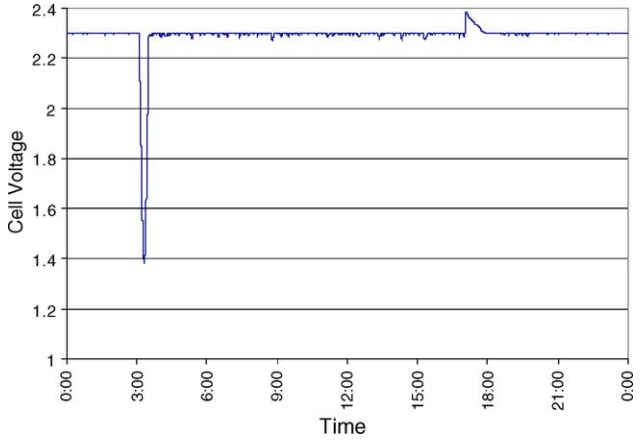

Fig. 14. Ultra capacitor cell voltage for 0.1 kWs^{-1}—demand sizing scenario.

perturbations while using more of the ultra capacitor system capacity. This is shown for example by the plot of cell voltage for 0.1 kWs^{-1} fuel cell ramp rate case in Fig. 14, which verifies that the ultra capacitor bank was more appropriately sized for this demand profile. This suggests that demand based sizing of ultra capacitor systems will have a significant effect in helping to reduce the dynamic ramping rate requirements of HTFC's, as the necessary amount of EES can be greatly reduced. Additionally, this result shows that building demand control, such as limiting instantaneous load changes experienced by air conditioning and other large loads, will have a profound impact on fuel cell systems' abilities to serve off-grid buildings and minimize utility grid instabilities.

The economics for the building demand sizing design scenario prove to be much more favorable over a broad range of HTFC ramp rates when compared with the worst-case design scenario (Table 2). For this analysis, the HTFC and ultra capacitor costs were assumed to be US$ 4000 kW^{-1} and US$ 100 $cell^{-1}$, respectively. For the worst-case design scenario, the EES increases the overall system cost by 17% when the HTFC ramp rate is 1 $kW\,s^{-1}$. However, when the EES is sized specifically for the demand, the ultra capacitor bank increases the overall cost by less than 5% for the 1 kWs^{-1} fuel cell ramp rate case, reinforcing the notion that building specific EES sizing and demand management will play important roles in helping to ease the ramping requirements of high temperature fuel cell systems.

5. Conclusions

The results from this study give insight into the dynamic requirements of stationary high temperature fuel cell (HTFC) systems for meeting the transients of measured commercial building loads when integrated with ultra capacitors as an electrical energy storage medium. In the framework of most current utility grid rate schedules, there is little economic incentive to increase HTFC ramping capability beyond 1 kWs^{-1}. However, this will come at the possible expense of grid stability (spikes in power to/from the utility grid), which will increase the resistance of utility companies to widespread HTFC adoption. Grid-parallel HTFC systems without EES will not be able to satisfy highly dynamic loads without utility grid perturbation unless their ramping rate approaches or exceeds 100 kWs^{-1} (40% s^{-1}), a target which appears unlikely today. In the context of stand-alone operation or elimination of utility grid perturbations, the use of ultra capacitors with HTFC systems is limited due to the inherent low energy storage density of ultra capacitors. However, ultra capacitors are feasible for integration with HTFC's as long as ramping rates approach 10 kWs^{-1} (4% s^{-1}), based on a worst-case design approach for a 250 kW HTFC system. By leveraging understanding of the end-use demand profile and through use of demand control techniques, the HTFC ramping rate required for feasible ultra capacitor integration can be reduced to 1 kWs^{-1} or slower, a much more reasonable target for HTFC dynamic load-following capability.

Acknowledgement

The U.S. Department of Defense Fuel Cell Program provided financial support for this research under Contract Number DACA42-02-C-0053. We gratefully acknowledge the contract manager, Frank Holcomb, for his technical contributions and insights.

References

[1] California Stationary Fuel Cell Collaborative, White Paper Summary of Interviews with Stationary Fuel Cell Manufacturers. http://stationaryfuelcells.org, August 2003.

[2] A.J. Leo, A.J. Skok, T.P. O'Shea, Santa Clara direct carbonate fuel cell demonstration, in: Proceedings of the FETC Fuel Cells '97 Review Meeting, 26–28 August, 1997.
[3] A. Burke, Ultracapacitor: why, how, and where is the technology, J. Power Sources 91 (2000) 37–50.
[4] D.Y. Jung, Y.H. Kim, S.W. Kim, S.H. Lee, Development of ultracapacitor modules for 42-V automotive electrical systems, J. Power Sources 114 (2) (2003) 366–373, 12 March.
[5] G. Pede, A. Iacobazzi, S. Passerini, A. Bobbio, G. Botto, FC vehicle hybridisation: an affordable solution for an energy-efficient FC powered drive train, J. Power Sources 125 (2) (2004) 280–291.
[6] A. Drolia, P. Jose, N. Mohan, An approach to connect ultracapacitor to fuel cell powered electric vehicle and emulating fuel cell electrical characteristics using switched mode converter, Industrial Electronics Society, in: IECON '03. The 29th Annual Conference of the IEEE, vol. 1, 2–6 November, 2003, pp. 897–901.
[7] T.A. Nergaard, J.F. Ferrell, L.G. Leslie, Jih-Sheng Lai, Design considerations for a 48 V fuel cell to split single phase inverter system with ultracapacitor energy storage, in: Power Electronics Specialists Conference, 23–27 June 2002, IEEE 33rd Annual, vol. 4, 2002, pp. 2007–2012.
[8] C. Wallmark, P. Alvfors, Technical design and economic evaluation of a stand-alone PEFC system for buildings in Sweden, J. Power Sources 118 (1–2) (2003) 358–366.
[9] D.H. Archer, J.G. Wimer, M.C. Williams, A phosphoric acid fuel cell cogeneration system retrofit to a large office building, in: Proceedings of the 32nd Intersociety, vol. 2, Energy Conversion Engineering Conference, 27 July–1 August, 1997, pp. 817–824.
[10] S.R. Torres, FuelCell Energy's Carbonate Technology Proceedings of the 2003 Fuel Cell Technology Institute, 23–24 June, 2003.
[11] D. New, J.G. Kassakian, J. Schindall, Automotive Applications of Ultracapacitors, MIT/Industry Consortium on Advanced Automotive Electrical/Electronic Components and Systems, Consortium Project Report Winter 2003.
[12] J.M. Miller, P.J. McCleer, M. Cohen, Ultracapacitors as Energy Buffers in a Multiple Zone Electrical Distribution System, www.maxwell.com.
[13] M.H. Todorovic, L. Palma, et al., Design of a wide input range DC–DC converter with a robust power control scheme suitable for fuel cell power conversion, in: Applied Power Electronics Conference and Exposition, APEC '04. Nineteenth Annual IEEE, 2004.